A human iPSC derived bone marrow milieu identifies a novel target against niche-conferred leukaemia proliferation and treatment resistance

Pal, Deepali*[a1,2], Blair, Helen[a1], Boyd, Sophie[1], Angel Hanmy Sharon[1,10], Nizami, Salem[1]., Isa, Asmida[1,9]., Beckett, Melanie[1]., Nelson, Ryan[1,3], Wilson, Aaron[1], Singh, Mankaran[1]., Sankar, Shalini[1,4]., Tirtakusuma, Ricky[1,5]., Sirintra, Nakjang[1]., Knill, Carly[6]., Fuller, Andrew[6]., McNeill, Hesta[1]., Russell, Lisa[1]., Schwab, Claire[1]., Zhous, Peixun[1]., Sinclair, Paul[1]., Coxhead, Jonathan[8]., Filby, Andrew[6]., Halsey, Christina[9]., Allan, James,M.[1], Harrison, J. Christine[1]., Moorman, Anthony[1]., Heidenreich Olaf.[b,1,3] Vormoor, Josef[b,1,3].

*Correspondence to Pal,D. at deepali.pal@northumbria.ac.uk

[a]: joint first

[b]: joint last

Affiliations

1. Wolfson Childhood Cancer Research Centre, Translational and Clinical Research Institute, Faculty of Medical Sciences, Newcastle University, Herschel Building Level 6, Brewery Lane, Newcastle upon Tyne, NE1 7RU. UK.
2. Department of Applied Sciences, Room A105, Ellison Building, Northumbria University, Newcastle upon Tyne, NE1 8ST. UK.
3. Princess Maxima Centrum for Pediatric Oncology, Heidelberglaan 25, 3584CS Utrecht. The Netherlands.
4. Division of Cancer Sciences, Oglesby Cancer Research Building, The University of Manchester, 555 Wilmslow Rd, Manchester, M20 4GJ, UK
5. Vall d'Hebron Institute of Oncology, Carrer de Natzaret 115, Lab 4.04A, 08035, Barcelona. Spain.

[6] Flow Cytometry Core Facility, Biosciences Institute, William Leech Building, 2nd floor Room M2.099, The Medical School, Framlington Place, Newcastle University, Newcastle upon Tyne, NE2 4HH. UK.

[7] Genomics Core Facility, Newcastle University, International Centre for Life, Central Parkway, Newcastle upon Tyne, NE1 3BZ. UK.

[8] Wolfson Wohl Cancer Research Centre, Institute of Cancer Sciences, College of Medical, Veterinary and Life Sciences, University of Glasgow, Garscube Estate, Switchback Road, Bearsden, Glasgow, G61 1QH. UK.

[9] Advanced Medical and Dental Institute, Universiti Sains Malaysia, Bertam 13200 Kepala Batas, Pulau Pinang Malaysia

[10] Faculty of Medicine, Universitas Indonesia, Indonesia

Abstract

Detecting how to clinically target the leukaemia microenvironment has remained a substantial hindrance in drug discovery and drug development. To address this clinical challenge, we have developed a human pluripotent stem cell-engineered co-culture system to support the *ex vivo* propagation of patient-derived leukaemia cells and to explore actionable niche-mediated blood cancer biology. Here we show that both messenchymal and vascular niche cell types impact malignant proliferation, dormancy and treatment resistance. Furthermore, both the niche cell types supported blast proliferation and conferred dexamethasone resistance onto patient-derived leukaemia cells. While vascular cells protected only quiescent blasts against dexamethasone, mesenchymal cells protected both proliferating and dormant blasts. Growth support and treatment protection was dependent on direct cell-cell interaction and was mediated by N-cadherin (CDH2). We show that CDH2 antagonist ADH-1, a compound with a proven low toxicity profile in adult solid tumour Phase I trials showed high in vivo efficacy in a highly aggressive and incurable leukaemia patient-derived xenograft model. Furthermore, we observed superior *in vivo* efficacy of ADH-1/Dexamethasone combination compared with single agent Dexamethasone therapy. These findings provide a proof-of-concept

starting point to begin investigations into novel and potentially safe anti-cancer therapeutics that target actionable niche-mediated cancer cell dependencies in haematological malignancies.

200 words

Introduction

Treatment resistance remains a major obstacle in cancer management. Emerging evidence suggests that in addition to cell intrinsic mechanisms factors such as the cancer microenvironment is a major culpable factor in mediating cancer cell biology including response to therapy[1-4]. In direct contrast to the classical stem cell theory, which endows properties of quiescence and self-renewal to a rare hierarchical population of stem cells[5], recent studies attribute the microenvironment at least in certain tissues to function as mediators of stem cell self-renewal and differentiation[6,7]. Consequently, stem cell progenies enter “neutral competition” for vacant niche space and their fate is directly regulated by availability of an appropriate microenvironment[8,9]. In addition, it is now well documented that cancer cells evolve their surrounding microhabitat and this dynamism not only enhances malignant propagation but also provides a safe haven against chemotherapy[10,11]. One mechanism by which the niche has been reported to confer treatment resistance is through organelle transfer between cancer and niche cells mediated through direct cell contact[12]. For example, nanotubule formation resulting in transfer of mitochondria, autophagosomes and cell adhesion transmembrane protein ICAM1 from leukemia cells towards surrounding mesenchymal stem cells has been suggested as a potential mechanism by which cancer cells seek

protection from their niche[13]. Nevertheless, means of directly drugging such cell contact dependent treatment resistance through safe therapeutic agents are lacking. Furthermore, limited availability of tractable and patient-derived human cell based models[14,15] hinder the in-depth scrutiny of this intricate, multicomponent and continually evolving oncogenic milieu.

Using the bone marrow as a paradigm we microengineered human niche constituent cell types to define druggable cancer-niche interactions in patient-derived leukemic blasts. We applied our human cell-based approach to identify a novel means of drugging the cancerous niche. CDH2 is a cell adhesion molecule known to regulate stem cell fate and proliferation[16]; however, its role as a therapeutic target against malignant propagation and niche-mediated treatment response remains unexplored, particularly in childhood leukaemias. ADH-1(Exherin™) is a compound that has been proven to have a low toxicity profile in adult solid tumour clinical trials[17]. Here we validate CDH2 as an actionable target in leukaemia. Moreover our study highlights the opportunity to clinically repurpose ADH-1 (Exherin™), a drug that directly targets niche-mediated malignant propagation and survival/drug resistance.

Key Methods:

Patient samples:

Patient-derived leukaemia blasts were obtained from the Newcastle Biobank (REC reference number 07/H0906/109+5). Samples obtained from UCL were made under Research Ethics Committee reference 14/EM/0134.

Mouse xenograft studies:

All mouse studies were carried out in accordance with UK Animals (Scientific Procedures) Act, 1986 under project licence P74687DB5 following approval of Newcastle University animal ethical review body (AWERB). Mice were housed in specific pathogen free conditions in individually ventilated cages with sterile bedding, water and diet (Irradiated No. 3 breeding diet, SDS). Mice were checked daily to ensure good health. All procedures were performed in a laminar flow hood except bioluminescent imaging (BLI).

NSG mice (NOD.Cg-Prkdc^{scid} Il2rg ^{tm1Wjl}/SzJ) aged between 12 and 16 weeks, both male and female, from in-house colonies were used for transplantions. Mice were checked daily, weighed and examined at least once weekly during studies to ensure good health.

Results

1. BM-iPSC form leukaemia supporting mesenchymal and vascular bone marrow niches

In order to model the human leukaemia niche *ex vivo* we re-programmed primary bone marrow mesenchymal stroma cells to pluripotency. This provided us with a replenishable and well defined source of bone marrow constituent cells that would represent both the mesenchyme and vasculature. Sendai virus is a highly efficient approach most commonly utilised for pluripotent reprogramming however there are limitations to this technique[18]. Most RNA-based approaches require repeat transfections due to reprogramming factor mRNA degradation[19]. In light of this we adopted an RNA replicon reprogramming technology[18] that uses POU5F1, KLF4, SOX2 in combination with GLIS1 thereby replacing MYC and consequently endorsing a re-programming technology that is both virus and oncogene-free. Through standardised xeno-free protocols (Fig. 1. A) we engineered 13 immortalised BM-iPSC lines (Fig.S1-4). Microsatellite DNA fingerprinting against parental mesenchymal cells confirmed authenticity (Fig. S5) whilst gene expression profiling revealed up-regulation of the embryonic stem cell genes SOX2, NANOG, GDF3, TERT, DNMT3B, CDH1, POU5F1 and ZFP42 (Fig. S6). BM-iPSC showed pluripotent stem cell morphology and expressed embryonic stem cell and

pluripotency markers alkaline phosphatase, POU5F1, SOX2, SSEA4 and TRA-1-60 (Fig. 1.B., S7). *In vitro* embryoid bodies (Fig. S8) and *in vivo* teratomas demonstrating ectodermal, mesodermal and endodermal germ layers (Fig. 1. D.) further confirmed the pluripotent nature of BM-iPSC at functional level.

Next we differentiated Messenchymal (iMSC) and vascular (iANG) niche cells (together i-niche) from BM-iPSC through a mesoderm intermediate. Within 72 hours of initiating mesoderm induction, tightly packed pluripotent cells with high nuclear to cytoplasmic ratio began to alter their morphology to form cobblestone clusters comprised of polygonal cells (Fig. S9). Gene expression profiling confirmed downregulaton of pluripotent (Fig. S10) and upregulation of mesodermal genes (Fig. 1.E) thus corroborating directed differentiation of BM-iPSC into mesodermal lineage. Furthermore, we observed activation of Wnt signalling pathway during this process which was indicated by upregulation of WNT5A. WNT5A is observed in human embryonic stem cell-derived mesoderm[20] and upregulation of this gene confirms lineage-specific directed differentiation of BM-iPSC (Fig. S11). We further differentiated these early mesoderm cells into iMSC and iANG that exhibited clearly distinct transcriptomic patterns with iMSC upregulating mesenchymal genes (Fig. 1.F, Fig. S.12). Differentiation of iMSC into osteogenic, chondrogenic and

adipogenic cells (Fig. 1.G-H) further confirmed their mesenchymal stem or progenitor potential. We showed that iANG cells contained a known population of $CD31^+$ endothelia-like cells and $CD31^-$ perivascular-like cells (Fig. 1.I, S12,13). We further confirmed that CD31+ cells upregulated expression of genes such as APOE which has been documented to be localised to endothelial cells *in vivo*[21], VCAM1 which is an endothelial cell surface glycoprotein[22,23], CX3CL1 known to be produced by endothelial cell membranes[24,25] and OCLN, which has been documented as a functional marker of endothelial cells especially linked to their ability of tune formation[26]. We revealed that CD31- cells on the other hand expressed genes more closely associated with perivascular cells such as ANXA5[27], ITGB1[28] and HIF1A[29].

2. Niche–primed leukemia cells upregulate CDH2.

In order to specify the role of iMSC and iANG in sustaining haematopoiesis, we isolated CD45+ cells (Fig S.14) from non malignant human bone marrow tissues so as to co-culture these cells on iMSC and iANG. We showed that unlike microenvironment-free suspension cultures, both types of niche cells supported viability and proliferation of human haematopoietic cells (n= 3 patients) unlike microenvironment-free suspension cultures (Fig.2.A). To further define the clinical relevance of i-niche cells we evaluated and characterised its potential to re-create a

microenvironment that would support oncogenic survival, self-renewal and proliferation. To this end we confirmed the proliferation of blasts from several patient leukaemia samples (n=14 patients) on i-niche. In the first instance we showed blast supporting parity between primary MSC and iMSC (Fig S.15.). Next we cultured 13 different patient leukaemia samples(all collected at diagnosis, Table S1, Fig 2.B) *ex vivo* on the i-niche cells. We showed that direct niche contact was superior in supporting leukaemia proliferation compared to feeder-conditioned media (Fig S16). Using FISH analysis we validated retention of baseline chromosomal translocation on both i-niche cells(S17). Through whole exome sequencing experiments we further demonstrated maintenance of > 99% genomic complexity on both iMSC and iANG (Fig. S18). In order to define the role of the i-niche in lineage plasticity we first demonstrated a >5-fold fold expansion of a primary mixed lineage leukaemia sample on both iMSC and iANG (Fig.S.19, S.20). This patient (table S1) presented with t(4;11) leukaemia, with a $CD34^{+}CD19^{+}CD33^{+}CD15^{-}$ lymphoid immunophenotype at presentation and following 5 months of treatment on the Interfant 06 protocol a myeloid $CD34^{+}CD19^{-}CD33^{+}CD15^{+}$ immunophenotype at relapse. CD34, a transmembrane glycoprotein is a known marker for haematopoietic stem and progenitor cells[30]. We showed that both iMSC- and iANG- primed blasts retained higher CD34 expression as compared to parallel niche-free suspension cultures. In

addition, we revealed that both iMSC and iANG primed blasts retained expression of lymphoid marker CD19. On the contrary iMSC-primed blasts lost expression of myeloid marker CD33. We further found that iANG-primed blasts retained a myeloid immunophenotype, with a population of cells retaining CD33 and an emerging population of $CD15^{+}$ blasts. Taken together here we showed that both i-niche cells supported blasts expressing the haematopoietic stem cell marker CD34. We further showed that there was a propensity for lymphoid differentiation on both i-niche cells. In addition, leukaemic cells propagating on iMSC lost expression of myeloid markers; whereas blasts expressing myeloid lineage markers were maintained by the iANG niche cells.

In a previous study we confirmed that cell-cell contact between primary bone marrow mesenchymal stem cells and leukaemia cells played a significant role in supporting blast proliferation[15]. In order to further specify niche primed leukaemia behaviour, we conducted gene expression profiling with a focus on adherens junction molecules via a combined approach of RNA sequencing, qPCR arrays and real-time qPCR experiments on iMSC and iANG primed patient-blasts from a total of 7 different patient-derived leukaemia samples(6 diagnostic and 1 relapse sample). Following priming of the cancer cells by its microenvironment we observed changes in several genes relating to adherens junction

molecules, WNT and β-Catenin pathway genes (Fig. S21). Given our consistent observation that niche-mediated leukaemia survival and proliferation is regulated by direct cell contact, we further confirmed upregulation of several cell-cell junction and cell adhesion molecules on leukaemia blasts that were co-cultured with i-niche over seven days. These blasts were then harvested from co-cultures and following cell separation through filtration subjected to gene expression profiling experiments. Most specifically we found consistent upregulation of cell adhesion molecule CDH2 in i-niche primed blasts across two patient leukaemia samples (Figure 2.C, Figure S22). We further validated upregulation of CDH2 on a total of

7 patient samples, 6 of which were obtained from patients at diagnosis and one from relapse (Figure 2.D.).

3. Under Dexamethasone treatment pressure CDH2 is upregulated by iMSC-primed cycling cells.

In order to evaluate the role of CDH2 in niche-cell mediated cancer proliferation and quiescence, we focussed our attention on a t(17;19) B-ALL case (Table S1). At presentation, this patient was sensitive to steroid treatment but on relapse a homozygous deletion of the glucocorticoid receptor (encoded by NR3C1) resulted in resistance to Dexamethasone. DNA labelling dyes allow isolation and tracking of dormant cells identified

as the slow cycling label retaining population[31]. We performed cell generational tracing experiments to investigate patterns of dormancy between the mesenchymal and vascular microenvironments (Fig S23). We started our investigation with therapy naïve diagnostic patient-leukaemia cells and observed distinct patterns of cell division on the two niches (Figure 3.A.). We found that iMSC function was restricted to supporting the actively dividing blasts (label^{low}). In contrast, nearly 50% of the total patient-blasts growing on the iANG cells were in a non dividing (label^{high}) state. Both iMSC and iANG primed blasts engrafted immunocompromised mice although b-iANG cells were restricted to the mouse bone marrow with reduced splenic involvement (Fig.3.B., Table.S2.). It is well documented that quiescent and primitive haematopoietic stem cells home in to the endosteal perivascular niche[32] and remain confined within the bone marrow. Hence it may be likely that iANG-primed leukemic blasts show greater quiescent tendencies and thus remain confined to the bone marrow *in vivo*. To further define the role of niche in blast quiescence we extended our analysis to include cells from the matched relapse sample (Fig. 3.C-3E). We noted that the cells from the sample at diagnosis cycled twice as more on iMSC than iANG; however the cells at relapse cycled more on the iANG cells (Fig. 3C). Hoechst/Pyronin Y staining experiments showed a 4 fold higher G0 cell fraction in the relapse sample when compared against dexamethasone

sensitive diagnostic cells (Fig. 3.D). Furthermore, we found that at diagnosis twice as many G0 blasts were observed on iANG in contrast to the mesenchyme primed blasts. Of note, the % G0 within vascular primed blasts, (b-iANG) at diagnosis was identical to % G0 observed on both mesenchymal and vascular niche at relapse. In keeping with this, we observed that cell cycling patterns of the relapse cells were also very similar on both iMSC and iANG (Fig. 3.E.).

In order to further assess treatment resistance conferred by the i-niche cells, we repeat the cell division tracing under treatment pressure. Firstly, we confirmed dexamethasone response in keeping with clinical data: positive response on the sample at diagnosis and no response at dexamethasone-resistant relapse (Figure S24). Dose response curves demonstrate reduced sensitivity against dexamethasone on both the i-niche cells in direct contrast with the niche-free suspension cultures (Figure 3.F.). Furthermore, on iANG-niche cells dexamethasone treatment actively killed the dividing blasts leaving the non-dividing label^{high} population intact (Fig. 3.G). On iMSC, treatment caused the cell division curve to shift to the right depicting cell populations that were slower cycling and we found that this was further accompanied by emergence of a small non dividing population (label^{high}, 5%) (Fig. 3.H). In summary, slow cycling label^{high} blasts constituted nearly 50% of total

leukemia burden on the iANG niche - these survived dexamethasone treatment. iMSC niche also conferred protection against dexamethasone despite the absence of non-dividing cells suggesting that treatment resistance is unlikely to be attributed to dormancy alone. We revaluated the role of CDH2 in proliferation and treatment resistance and using 4 different patient-derived leukaemia samples showed that label^{low}, fast cycling iMSC-primed blasts that survive under dexamethasone pressure expressed higher levels of CDH2(Figure 3I, S25). On the contrary, we found that CDH2 expression to be very similar between fast and slow cycling (label^{high} versus label^{low}) dexamethasone resistant iANG-primed blasts (Fig.3.I). These results suggest that CDH2 plays an important role in mediating niche-dependent leukaemia proliferation in blasts that survive treatment with Dexamethasone.

4. CDH2 drives leukaemia proliferation and reduces sensitivity against Dexamethasone

In order to validate the function of CDH2 we performed RNAi knockdown experiments on both cancer cells and i-niche cells. CDH2 knockdown in 4 different leukaemia cell lines (Fig.4.A., Fig. S26, S27) resulted in reduced proliferation in four different leukemia cell lines (Fig. 4.B, 4C) in niche-free suspension cultures. We further detected that CDH2 knockdown in these leukaemia cells resulted in downregulation of a range of cancer

associated transcription factors and genes (Fig. S.28-S31) including several oncogenic pathways such as JAK-STAT, prolactin, chemokine and ErbB signalling (Figure S.29-S30) as well as modulation of several transcription and chromatin remodelling factors (Fig S31).

We found that when the $CDH2^{-}$ leukaemia cells were co-cultured using modified culture conditions to facilitate niche-dependence, they failed to survive on iMSC cells and further showed reduced proliferation when co-cultured with iANG (Fig 4.D). Furthermore, following CDH2 knockdown in iMSC(Fig 4.E), $iMSC^{CDH2-}$ deteriorated in their ability to support the proliferation of three different patient-derived leukaemia samples and one additional patient-derived leukaemia sample at relapse(Figure 4.F). Importantly, cancer blasts demonstrated 3 folds higher sensitivity to dexamethasone on $iMSC^{CDH2-}$ cells (Fig. 4.G) potentially suggesting that a protective role of CDH2 is conferred by the mesenchymal stem cells in the bone marrow.

Taken together, these data indicate that CDH2-mediated cancer proliferation could be dependent on both cell intrinsic mechanisms as well as cell extrinsic factors such as those mediated by cancer cell interactions with its surrounding niche cells.

5. CDH2 antagonist ADH-1 a repurposed compound shows high efficacy on a wide range of patient derived leukaemia cells

ADH-1 is a small, cyclic pentapeptide with the formula N-Ac-CHAVC-NH2 that competitively blocks the action of CDH2. It has additional antiangiogenic properties in disrupting tumour vasculature and inhibiting tumour growth. The compound has been in Phase I trials for advanced solid malignancies with outcome indicating a well tolerated toxicity profile[17]. However, its efficacy in blood cancers remains unknown. We applied our i-niche co-culture platform and demonstrated drug dose response of ADH-1 on 15 different patient-derived leukaemia samples (Fig. 5.A; Figure S32, Table S1). ADH-1 doses used throughout this study have been in compliance with plasma level concentrations that have been achieved in solid tumour trials[33]. We found that ADH-1 treatment showed maximum efficacy when the cancer cells were in direct contact with the niche as opposed to transwell co-cultures(Fig.5.C-D). We therefore show that a likely mechanism of ADH-1 action includes disruption of cell-cell contact between leukaemia cells and i-niche. In addition, ADH-1 treatment increased leukaemia cell death as evidenced by increased Annexin V, PI staining (Figure 5.E). To further investigate the effect of this compound on cells that survive under treatment pressure we performed live cell cycle and G0 analysis on patient-blasts at relapse. We found that ADH-1

treatment minimised patient-blast-proliferation as evidenced by reduced S phase whilst demonstrating no increase in % G0 cells(Figure 5.F). Taken together this data corroborates that ADH-1 is a promising candidate to reduce the tumour burden in treatment resistant relapse without any associated increase in quiescent cell fractions.

Despite the recent improvements in biology driven therapeutics single agent treatment has been associated with emergence of treatment resistant cancer clones[34,35]. Combinatorial drug treatment is therefore a central principle in anti-cancer therapeutic regimens to enhance efficacy through drug synergies and mitigate emergence of treatment resistance. We performed drug combination assays of Dexamethasone-ADH1 combination using a total of four different patient-derived leukaemia samples co-cultured on i-niche cells(Fig. 6.A-F) and found synergistic interaction as analysed by the principles of the Bliss Independence model. Subsequently, we conducted further comprehensive drug matrix analysis (Fig. 6F-G) and showed that ADH-1 demonstrates synergy in combination with clinically relevant concentrations of Dexamethasone achieving ZIP synergy scores of >10 on both iMSC and iANG. Consequently, we now initiated studies to explore if ADH-1/Dexamethasone combination would demonstrate efficacy *in vivo* using an orthotopic patient derived xenograft model.

6. ADH-1 shows high *in vivo* efficacy both as a single agent and in combination with Dexamethasone in very high risk incurable leukaemia

In order to validate the function of CDH2 *in vivo*, we interrogated leukaemia initiation and propagation blasts using an orthotopic patient derived xenograft, PDX, model previously developed by us[36,37]. We transplanted luciferase-tagged leukaemic blasts harvested from a clinical sample of very high risk and incurable acute lymphoblastic leukaemia (ALL sample, L707, Table S1) directly into the bone marrow of immunodeficient mice. We monitored leukaemic engraftment into the mouse bone marrow through bioluminescence signal and we further confirmed successful engraftment through immunohistochemistry staining of mouse bone marrow with human CD19 (a lymphoid cell marker) (Fig. S33). In an initial pilot we treated mice with a combination of ADH-1 and dexamethasone to determine a non-toxic dose and schedule for further study (Fig S34.A.). This small-scale dose escalation pilot study indicated that ADH1/Dexamethasone in combination significantly reduced leukaemic engraftment (Figure S34.B) thereby justifying further *in vivo* investigation of the combination treatment. We also found that ADH1/Dexamethasone [ADH1 200mg/kg; Dexamethasone 3mg/kg] delivered via intraperitoneal injection was well tolerated when

administered 5 times weekly for 3 weeks with minimal weight loss. Consequently, we selected ADH1 dose from the tolerated and efficacious doses applied previously in mice[38,39] and we chose a dexamethasone dose to replicate plasma concentrations achieved in ALL patient therapy[33,40,41]. We repeated the *in vivo* transplantation experiments using bioluminescent tagged patient derived ALL blasts as described above and started drug dosing on day 6 following transplantation (Fig.7.A). As expected, we observed that dexamethasone slowed leukaemic growth but we further revealed that ADH-1 alone had a bioluminescent signal similar to mice administered with Dexamethasone. We also found that ADH1/Dexamethasone combination treatment profoundly reduced leukemic engraftment compared to controls and single agents. Through additional bioluminescent imaging (BLI) we demonstrated significantly lower overall signals compared to untreated controls at both weeks 2 and 3 of ADH1/Dexamethasone treatment (Fig 7B-C). Confirming the BLI data, we showed that spleen sizes were significantly smaller in the ADH1/Dexamethasone treated mice at the end of the study. We further showed that the proportion of leukaemic blasts in bone marrow and spleen was significantly less in ADH1/Dexamethasone treated mice compared to mice from dexamethasone and control groups (Fig 7D-E, S34-S35). In keeping with our *in vitro* observations, we showed that ADH1/Dexamethasone combination was most effective in the bone

marrow (7D-E) suggesting that a key mechanism of action for ADH-1 was to disrupt CDH2-mediated blast interactions and consequently increase sensitivity against dexamethasone. In summary, we found that treatment with only 15 doses of dexamethasone in the presence of ADH1 was more effective than dexamethasone alone at preventing leukaemic growth *in vivo*. This *in vivo* efficacy validated the use of our engineered preclinical model for the identification of exploitable niche targets.

Discussion:

Treatment resistance and treatment toxicity are major clinical challenges that urgently need more attention. Dynamism of the leukaemic niche and consequently its role in dormancy and treatment resistance is well documented[2,31,42-44]. Indeed, standard chemotherapy primes cancer and its ambiance alike endowing cell intrinsic and non-cell-autonomous adaptations towards treatment resistance[2,45]. Recent concepts such as non-oncogene addiction[34], a phenomenon underpinning cancer cell survival through exaggerated functioning of non-mutated genes have emerged as promising solutions to prevent treatment resistance. Despite the significant impacts of the niche on cancer cell function; no druggable niche targets exist that can directly impact microenvironment mediated leukaemia biology. Indeed, current day treatment largely disregards the

influence of the oncogenic microenvironment on malignant proliferation, self-renewal and treatment resistance.

To identify new and safer targets against the leukaemia niche we require patient-derived preclinical models. This is a major challenge in haematological malignancies since primary leukaemia cells do not proliferate once removed from the patient. Consequently, there is a lack of models that allow scrutiny of the niche in a human cell based and patient-derived setting[14,15]. Here we have shown that human pluripotent stem-cell engineered bone marrow cells support ex vivo proliferation of patient-derived leukaemia cells. Furthermore, we found that these niche cell types specify both proliferative and quiescent niches for leukemia (Fig.8).

The role of CDH2 in directing stem-cell fate, tumour-microenvironment interactions and chemoresistance has been implicated in a wide variety of solid tumours and certain haematological malignancies[46,47]. However, CDH2-mediated cancer proliferation remains unexplored as does directly targeting this molecule towards anti-leukaemia treatment. Here we have revealed novel insights into clinically actionable interactions of patient leukaemia blasts with both the mesenchymal and vascular cellular constituents of the haematopoietic niche. In line with the emerging concept that therapy-naïve leukaemic stem cells and post-therapy

treatment resistant leukaemia regenerating cells are distinct populations[31,45] we found that although a key association of treatment resistance remains dormancy, not all treatment resistant cells are dormant. Therefore, other mechanisms warrant attention. We observed that applying dexamethasone treatment pressure caused upregulation of CDH2 in mesenchyme primed proliferating blasts. Through functional validation assays on both blasts and niche cells we further confirmed that CDH2 mediates both blast proliferation and treatment response. We found that dexamethasone showed higher efficacy in killing patient derived leukaemia cells in $IMSC^{CDH2-}$ co-cultures. Together these findings highlight a key role of CDH2 and the bone marrow mesenchyme in simultaneously endowing malignant proliferation and treatment resistance. Mechanistically we showed that downregulation of CDH2 reduces blast-niche interactions. We further found that CDH2 knockdown also downregulates several cell intrinsic oncogenic pathways such as the JAK-STAT pathway. Ultimately, we confirmed that clinically relevant concentrations of the pentapeptide ADH-1[17], a functional antagonist of CDH2 showed high efficacy against a panel of 15 patient derived leukaemia samples. Subsequent *in vivo* validation confirmed that ADH-1 efficacy in an orthotopic mouse model of a highly aggressive incurable leukaemia was comparable to dexamethasone efficacy alone. Importantly, Dexamethasone-ADH1 combination showed superior

efficacy than treatment with Dexamethasone alone and the addition of ADH-1 did not increase treatment toxicity. Of note, data from clinical trials on solid tumours[17,33,48,49] indicate that ADH-1 has a well-tolerated toxicity profile. Based on these findings we reveal that ADH-1 would be of high translational significance as a repurposed agent in the treatment of blood cancers.

Using the complex haematopoietic bone marrow niche as a paradigm our proof-of-concept preclinical platform provides a prototype which can be adapted to investigate malignant niches in a wide variety of haematological cancer clinical samples. Our findings reveal new insights into therapeutically targeting the leukaemia microenvironment with promise to impact future treatment protocols towards safer and more efficacious therapies.

Word Count: 4000

Author Contributions:

DP conceived and designed the project, secured the major funding, organised conduct of the study, designed and carried out experiments, analysed and interpreted data and wrote the manuscript. HB contributed essential advice to project design, organised conduct of *in vivo* experiments, designed and carried out experiments, analysed and interpreted data and provided essential intellectual input in writing of the

manuscript. SB, AHS, SN and AW performed experiments, analysed data and contributed to data interpretation. AI, MB performed experiments, analysed and interpreted data and contributed to review and edit of manuscript. RN, MS, SS, RT, CK, AF, HMN, LR, CS, PZ, PS provided samples, performed experiments and analysed data. SN performed bioinformatics analysis. JC, AF contributed to experimental design and data analysis and interpretation. CJH, AM, CH and JA contributed to study organisation and critiqued the manuscript for important intellectual content. OH and JV provided funding, provided input with experimental design and critiqued the manuscript for important intellectual content. All authors approved the final version of the manuscript.

Acknowledgements:

This study was funded by NC3Rs through a fellowship to DP, CCLG through a project grant to DP, JV and OH and a Wellcome Trust NUSCU award to DP. We would like to further thank CRUK for a programme grant C27943/A12788 to JV and OH and NECCR for funding core infrastructure at Wolfson Childhood Cancer Research Centre, Newcastle University. The IVIS Spectrum was funded by grant 087961 from the Wellcome Trust. We thank Universiti Sains Malaysia and Kementerian Pengajian Tinggi Malaysia for funding PhD studentship to AI. We also thank Dr. Malgorzata

Firczuk, Medical University of Warsaw for the provision of leukaemia PDX samples.

Competing Interests statement:

No competing interests declared.

References:

1. Agarwal, P.*, et al.* Mesenchymal Niche-Specific Expression of Cxcl12 Controls Quiescence of Treatment-Resistant Leukemia Stem Cells. *Cell Stem Cell* **24**, 769-784 e766 (2019).
2. Duan, C.W.*, et al.* Leukemia propagating cells rebuild an evolving niche in response to therapy. *Cancer Cell* **25**, 778-793 (2014).
3. Guarnerio, J.*, et al.* A non-cell-autonomous role for Pml in the maintenance of leukemia from the niche. *Nat Commun* **9**, 66 (2018).
4. Zhang, B.*, et al.* Bone marrow niche trafficking of miR-126 controls the self-renewal of leukemia stem cells in chronic myelogenous leukemia. *Nat Med* **24**, 450-462 (2018).
5. Bonnet, D. & Dick, J.E. Human acute myeloid leukemia is organized as a hierarchy that originates from a primitive hematopoietic cell. *Nat Med* **3**, 730-737 (1997).
6. Batlle, E. & Clevers, H. Cancer stem cells revisited. *Nat Med* **23**, 1124-1134 (2017).
7. Doupe, D.P., Klein, A.M., Simons, B.D. & Jones, P.H. The ordered architecture of murine ear epidermis is maintained by progenitor cells with random fate. *Dev Cell* **18**, 317-323 (2010).
8. Lopez-Garcia, C., Klein, A.M., Simons, B.D. & Winton, D.J. Intestinal stem cell replacement follows a pattern of neutral drift. *Science* **330**, 822-825 (2010).
9. Snippert, H.J.*, et al.* Intestinal crypt homeostasis results from neutral competition between symmetrically dividing Lgr5 stem cells. *Cell* **143**, 134-144 (2010).
10. Akinduro, O.*, et al.* Proliferation dynamics of acute myeloid leukaemia and haematopoietic progenitors competing for bone marrow space. *Nat Commun* **9**, 519 (2018).
11. Duarte, D.*, et al.* Inhibition of Endosteal Vascular Niche Remodeling Rescues Hematopoietic Stem Cell Loss in AML. *Cell Stem Cell* **22**, 64-77 e66 (2018).
12. Mendez-Ferrer, S.*, et al.* Bone marrow niches in haematological malignancies. *Nat Rev Cancer* **20**, 285-298 (2020).
13. de Rooij, B., Polak, R., Stalpers, F., Pieters, R. & den Boer, M.L. Tunneling nanotubes facilitate autophagosome transfer in the leukemic niche. *Leukemia* **31**, 1651-1654 (2017).
14. Martinez-Soria, N.*, et al.* The Oncogenic Transcription Factor RUNX1/ETO Corrupts Cell Cycle Regulation to Drive Leukemic Transformation. *Cancer Cell* **34**, 626-642 e628 (2018).
15. Pal, D.*, et al.* Long-term in vitro maintenance of clonal abundance and leukaemia-initiating potential in acute lymphoblastic leukaemia. *Leukemia* **30**, 1691-1700 (2016).
16. Alimperti, S. & Andreadis, S.T. CDH2 and CDH11 act as regulators of stem cell fate decisions. *Stem Cell Res* **14**, 270-282 (2015).
17. Yarom, N.*, et al.* Phase I clinical trial of Exherin (ADH-1) in patients with advanced solid tumors. *Curr Clin Pharmacol* **8**, 81-88 (2013).
18. Yoshioka, N.*, et al.* Efficient generation of human iPSCs by a synthetic self-replicative RNA. *Cell Stem Cell* **13**, 246-254 (2013).
19. Warren, L.*, et al.* Highly efficient reprogramming to pluripotency and directed differentiation of human cells with synthetic modified mRNA. *Cell Stem Cell* **7**, 618-630 (2010).

20. Evseenko, D.*, et al.* Mapping the first stages of mesoderm commitment during differentiation of human embryonic stem cells. *Proc Natl Acad Sci U S A* **107**, 13742-13747 (2010).
21. Yue, L.*, et al.* Apolipoprotein E enhances endothelial-NO production by modulating caveolin 1 interaction with endothelial NO synthase. *Hypertension* **60**, 1040-1046 (2012).
22. Osborn, L.*, et al.* Direct expression cloning of vascular cell adhesion molecule 1, a cytokine-induced endothelial protein that binds to lymphocytes. *Cell* **59**, 1203-1211 (1989).
23. Rice, G.E. & Bevilacqua, M.P. An inducible endothelial cell surface glycoprotein mediates melanoma adhesion. *Science* **246**, 1303-1306 (1989).
24. Imaizumi, T., Yoshida, H. & Satoh, K. Regulation of CX3CL1/fractalkine expression in endothelial cells. *J Atheroscler Thromb* **11**, 15-21 (2004).
25. Szukiewicz, D.*, et al.* Fractalkine (CX3CL1) and its receptor CX3CR1 may contribute to increased angiogenesis in diabetic placenta. *Mediators Inflamm* **2013**, 437576 (2013).
26. Kanayasu-Toyoda, T.*, et al.* Occludin as a functional marker of vascular endothelial cells on tube-forming activity. *J Cell Physiol* **233**, 1700-1711 (2018).
27. Brachvogel, B.*, et al.* Perivascular cells expressing annexin A5 define a novel mesenchymal stem cell-like population with the capacity to differentiate into multiple mesenchymal lineages. *Development* **132**, 2657-2668 (2005).
28. Turlo, K.A.*, et al.* beta1-integrin is essential for vasoregulation and smooth muscle survival in vivo. *Arterioscler Thromb Vasc Biol* **33**, 2325-2335 (2013).
29. Qi, D.*, et al.* Hypoxia inducible factor 1alpha in vascular smooth muscle cells promotes angiotensin II-induced vascular remodeling via activation of CCL7-mediated macrophage recruitment. *Cell Death Dis* **10**, 544 (2019).
30. Steidl, U.*, et al.* Primary human CD34+ hematopoietic stem and progenitor cells express functionally active receptors of neuromediators. *Blood* **104**, 81-88 (2004).
31. Ebinger, S.*, et al.* Characterization of Rare, Dormant, and Therapy-Resistant Cells in Acute Lymphoblastic Leukemia. *Cancer Cell* **30**, 849-862 (2016).
32. Morrison, S.J. & Scadden, D.T. The bone marrow niche for haematopoietic stem cells. *Nature* **505**, 327-334 (2014).
33. Perotti, A.*, et al.* Clinical and pharmacological phase I evaluation of Exherin (ADH-1), a selective anti-N-cadherin peptide in patients with N-cadherin-expressing solid tumours. *Ann Oncol* **20**, 741-745 (2009).
34. Nagel, R., Semenova, E.A. & Berns, A. Drugging the addict: non-oncogene addiction as a target for cancer therapy. *EMBO Rep* **17**, 1516-1531 (2016).
35. Workman, P., Al-Lazikani, B. & Clarke, P.A. Genome-based cancer therapeutics: targets, kinase drug resistance and future strategies for precision oncology. *Curr Opin Pharmacol* **13**, 486-496 (2013).
36. Bomken, S.*, et al.* Lentiviral marking of patient-derived acute lymphoblastic leukaemic cells allows in vivo tracking of disease progression. *Leukemia* **27**, 718-721 (2013).
37. Elder, A.*, et al.* Abundant and equipotent founder cells establish and maintain acute lymphoblastic leukaemia. *Leukemia* **31**, 2577-2586 (2017).
38. Shintani, Y.*, et al.* ADH-1 suppresses N-cadherin-dependent pancreatic cancer progression. *Int J Cancer* **122**, 71-77 (2008).
39. Turley, R.S.*, et al.* Targeting N-cadherin increases vascular permeability and differentially activates AKT in melanoma. *Ann Surg* **261**, 368-377 (2015).
40. Matheson, E.C.*, et al.* Glucocorticoids and selumetinib are highly synergistic in RAS pathway-mutated childhood acute lymphoblastic leukemia through upregulation of BIM. *Haematologica* **104**, 1804-1811 (2019).
41. Jackson, R.K.*, et al.* Impact of dose and duration of therapy on dexamethasone pharmacokinetics in childhood acute lymphoblastic leukaemia-a report from the UKALL 2011 trial. *Eur J Cancer* **120**, 75-85 (2019).

42. Pal, D., Heidenreich, O. & Vormoor, J. Dormancy Stems the Tide of Chemotherapy. *Cancer Cell* **30**, 825-826 (2016).
43. Kumar, B.*, et al.* Acute myeloid leukemia transforms the bone marrow niche into a leukemia-permissive microenvironment through exosome secretion. *Leukemia* **32**, 575-587 (2018).
44. Baryawno, N.*, et al.* A Cellular Taxonomy of the Bone Marrow Stroma in Homeostasis and Leukemia. *Cell* **177**, 1915-1932 e1916 (2019).
45. Boyd, A.L.*, et al.* Identification of Chemotherapy-Induced Leukemic-Regenerating Cells Reveals a Transient Vulnerability of Human AML Recurrence. *Cancer Cell* **34**, 483-498 e485 (2018).
46. Mangolini, M.*, et al.* Notch2 controls non-autonomous Wnt-signalling in chronic lymphocytic leukaemia. *Nat Commun* **9**, 3839 (2018).
47. Mrozik, K.M., Blaschuk, O.W., Cheong, C.M., Zannettino, A.C.W. & Vandyke, K. N-cadherin in cancer metastasis, its emerging role in haematological malignancies and potential as a therapeutic target in cancer. *BMC Cancer* **18**, 939 (2018).
48. Beasley, G.M.*, et al.* Prospective multicenter phase II trial of systemic ADH-1 in combination with melphalan via isolated limb infusion in patients with advanced extremity melanoma. *J Clin Oncol* **29**, 1210-1215 (2011).
49. Beasley, G.M.*, et al.* A phase 1 study of systemic ADH-1 in combination with melphalan via isolated limb infusion in patients with locally advanced in-transit malignant melanoma. *Cancer* **115**, 4766-4774 (2009).

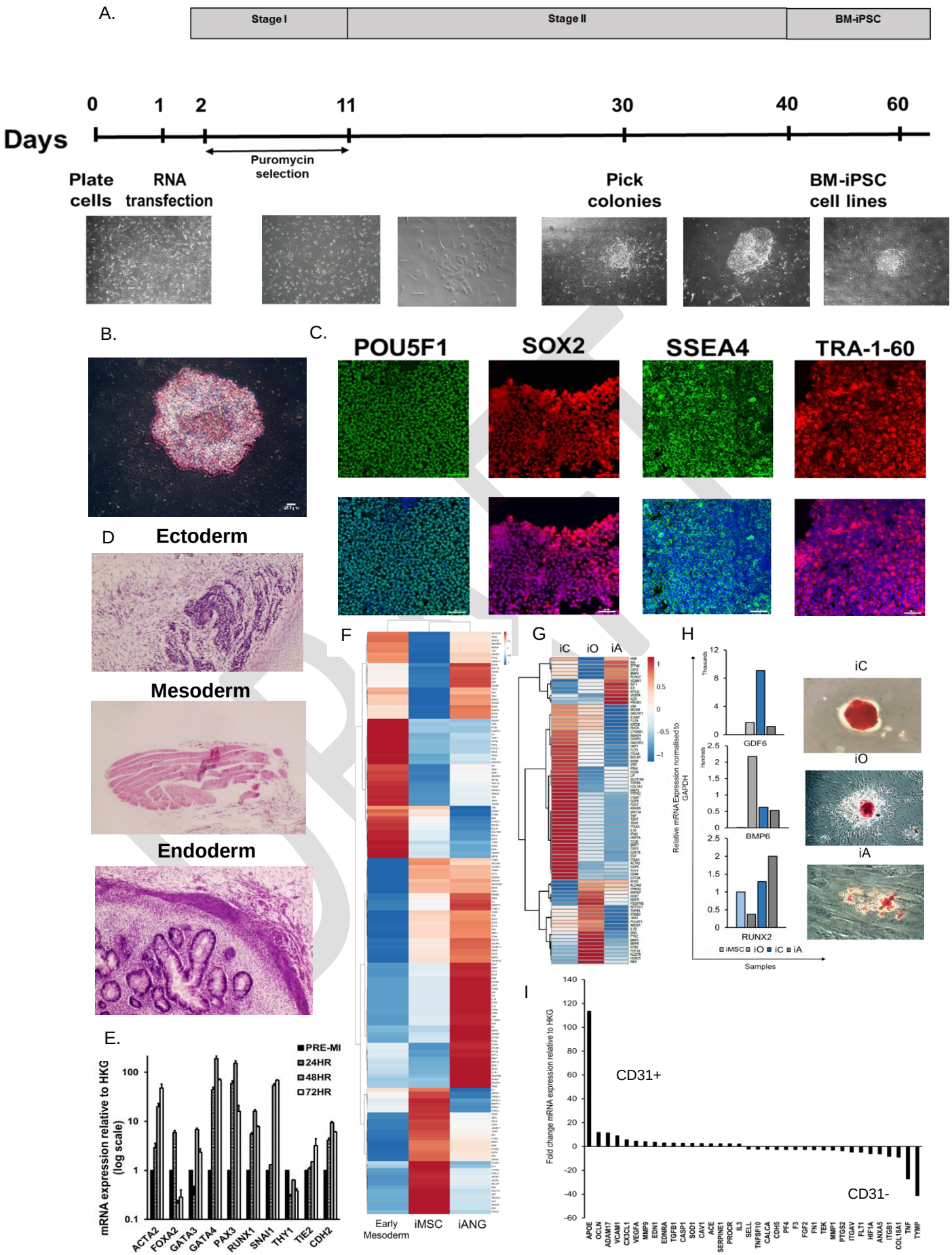
A.
Stage I
Stage II
BM-iPSC
Days
0
1
2
11
30
40
60
Puromycin selection
Plate cells
RNA transfection
Pick colonies
BM-iPSC cell lines
B.
C.
POU5F1
SOX2
SSEA4
TRA-1-60
D
Ectoderm
Mesoderm
Endoderm
E.
PRE-MI
24HR
48HR
72HR
mRNA expression relative to HKG (log scale)
ACTA2
FOXA2
GATA3
GATA4
PAX3
RUNX1
SNAI1
THY1
TIE2
CDH2
F
Early Mesoderm
iMSC
iANG
G
iC
iO
iA
H
GDF6
BMP6
RUNX2
Relative mRNA Expression normalised to GAPDH
Samples
I
CD31+
CD31-
Fold change mRNA expression relative to HKG

Figure 1. Virus and oncogene-free BM-iPSC form mesenchymal and vascular lineage through an intermediate early mesoderm route. A. Schema for synthetic RNA based re-programming using pluripotent transcripts POU5F1-SOX2-KLF4, GLIS1. B. Alkaline phosphatase staining in BM-iPSC. C. Nuclear POU5F1 and SOX2, cell surface SSEA4, TRA-1-60 staining in feeder-free and xeno-free cultures of BM-iPSC D. H&E staining of BM-iPSC-derived teratomas representing the three embryonic lineages. E. mRNA expression of BM-iPSC cells mesodermal differentiation at Pre-MI: pre mesoderm induction, 24, 48 and 72 hours of mesoderm induction stages. F. BM-iPSC derived early mesoderm, mesenchymal [iMSC] and vascular [iANG] cells demonstrate distinct transcriptomic profiles as evaluated by high throughput gene expression arrays G. iMSC differentiate into chondrocytes [iC], osteocytes [iO] and adipocytes [iA] with distinct gene expression profiles. H. GDF6, BMP6 and RUNX2 expression in iC, iO and iA. Immunohistochemical staining demonstrating Safranin O, Alizarin Red and Oil Red O staining in iC, iO and iA respectively. I. Gene expression profile in iANG containing representative vascular cells such as CD31+ endothelial cells [25%] and CD31- perivascular cells [75%] in known proportions. CD31+ cells express endothelia-relevant markers such as APOE, OCLN, ADAM17, VCAM1 whereas CD31- cells express perivascular markers such as ANXA5, ITGB1, HIF1A and COL18A1

DRAFT

A.

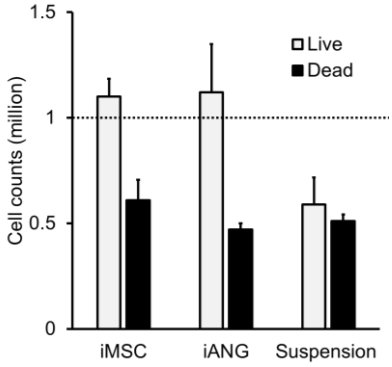
1.5
1
0.5
0
Cell counts (million)
Live
Dead
iMSC
iANG
Suspension

B.

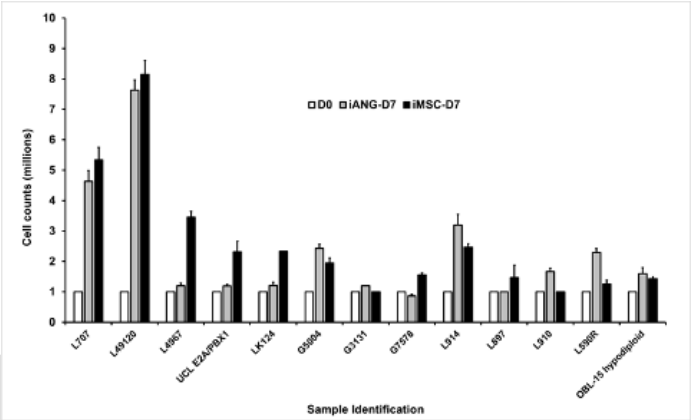
D0
iANG-D7
iMSC-D7
Cell counts (millions)
Sample Identification
L707
L49120
L4967
UCL E2A/PBX1
LK124
G5004
G3131
G7578
L914
L997
L910
L996R
GBL-15 hypodiploid

C.

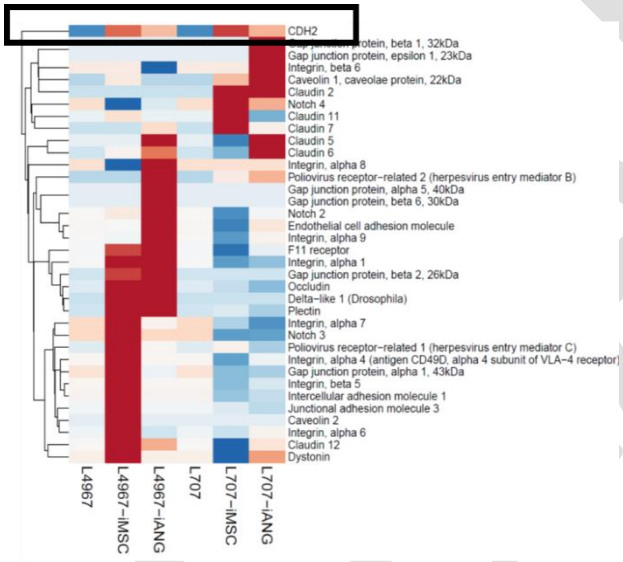
CDH2
Gap junction protein, beta 1, 32kDa
Gap junction protein, epsilon 1, 23kDa
Integrin, beta 6
Caveolin 1, caveolae protein, 22kDa
Claudin 2
Notch 4
Claudin 11
Claudin 7
Claudin 5
Claudin 6
Integrin, alpha 8
Poliovirus receptor-related 2 (herpesvirus entry mediator B)
Gap junction protein, alpha 5, 40kDa
Gap junction protein, beta 6, 30kDa
Notch 2
Endothelial cell adhesion molecule
Integrin, alpha 9
F11 receptor
Integrin, alpha 1
Gap junction protein, beta 2, 26kDa
Occludin
Delta-like 1 (Drosophila)
Plectin
Integrin, alpha 7
Notch 3
Poliovirus receptor-related 1 (herpesvirus entry mediator C)
Integrin, alpha 4 (antigen CD49D, alpha 4 subunit of VLA-4 receptor)
Gap junction protein, alpha 1, 43kDa
Integrin, beta 5
Intercellular adhesion molecule 1
Junctional adhesion molecule 3
Caveolin 2
Integrin, alpha 6
Claudin 12
Dystonin
L4967
L4967-iMSC
L4967-iANG
L707
L707-iMSC
L707-iANG

D

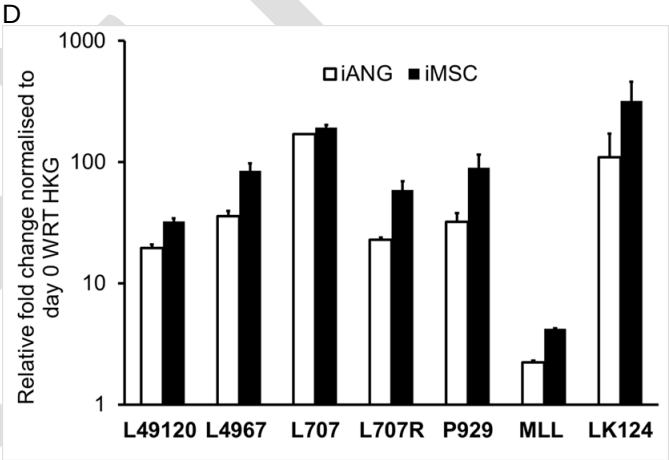
1000
100
10
1
Relative fold change normalised to day 0 WRT HKG
iANG
iMSC
L49120
L4967
L707
L707R
P929
MLL
LK124

Figure 2. Niche – primed leukemia cells upregulate CDH2. A. Cell counts of non malignant human haematopoietic cells on iMSC, iANG and in niche-free suspension cultures over 7 days. B. Cell counts of patient-leukemic blasts on iMSC and iANG at diagnosis and relapse over a seven day period. C. Heatmap demonstrating gene expression profiling of niche primed patient-leukemia samples [L707, L4967] shows consistent upregulation of CDH2 following co-culture with iMSC and iANG D. CDH2 upregulation confirmed on 7 leukaemia samples following a 7 day co-culture with iMSC and iANG

DRAFT

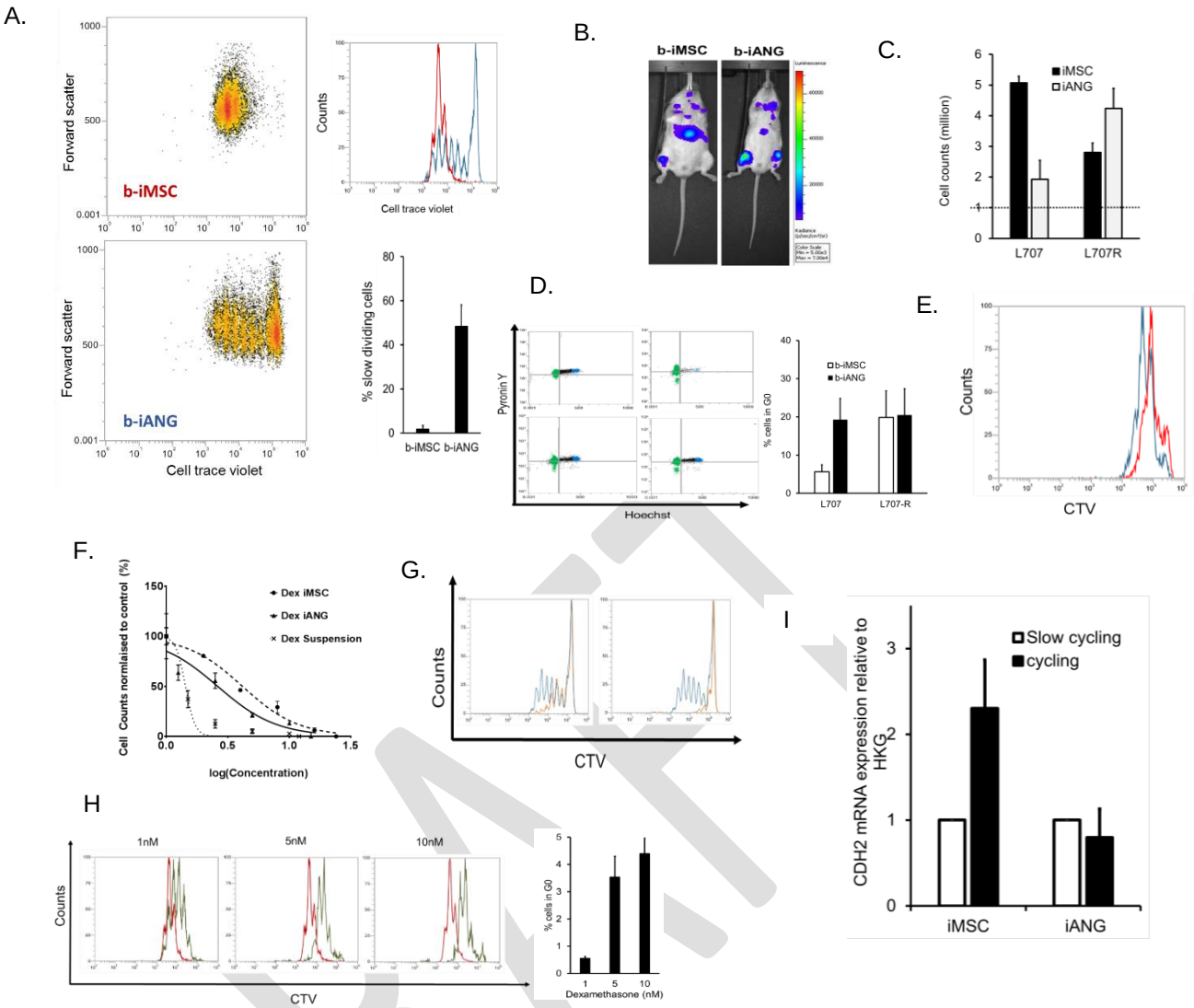
A.
Forward scatter
b-iMSC
b-iANG
Cell trace violet
Counts
% slow dividing cells
b-iMSC b-iANG
B.
b-iMSC
b-iANG
C.
iMSC
iANG
Cell counts (million)
L707
L707R
D.
Pyronin Y
Hoechst
% cells in G0
b-iMSC
b-iANG
L707
L707-R
E.
Counts
CTV
F.
Cell Counts normalised to control (%)
Dex iMSC
Dex iANG
Dex Suspension
log(Concentration)
G.
Counts
CTV
I
CDH2 mRNA expression relative to HKG
Slow cycling
cycling
iMSC
iANG

H
1nM
5nM
10nM
Counts
CTV
% cells in G0
Dexamethasone (nM)

DRAFT

Figure 3. Under Dexamethasone treatment pressure CDH2 is upregulated by iMSC-primed cycling cells. A. Dot plots show fast cycling and slow cycling iMSC primed blasts [b-iMSC, red] and iANG primed blasts [b-iANG, blue] at Day 7 from a patient-leukemic sample at diagnosis. Graph shows % slow cycling blasts on iMSC and iANG. B. Total fluorescence intensity of luciferase-tagged niche-primed patient leukemic blasts transplanted in immunocompromised mice [intrafemoral transplants]. C. Cell counts of a diagnostic and matched relapse sample on iMSC and iANG. D. Hoechst-pyronin Y analysis [dot plot] of patient leukemic blasts on iMSC [left panel] and iANG [right panel] in patient leukemic blasts at diagnosis [top panel] and relapse [bottom panel]. Graph shows percentage cells in G0 on iMSC [b-iMSC] and on iANG [b-iANG] at diagnosis [L707] and relapse [L707-R]. E. Fast and slow cycling niche primed blasts from relapse sample on iMSC [red] and iANG [blue] at Day 7. F. Dexamethasone dose response (nM) curve of patient leukemia cells in niche-free suspension culture and on iMSC and iANG G. Histogram shows cell generational curve of untreated [blue] and treated cells [orange]. H. Cell generation curves of patient leukemic cells untreated [red] and treated [green]. Column graph shows % slow cycling blasts on iMSC under Dexamethasone treatment. I. CDH2 expression under dexamethasone pressure in slow cycling and cycling/fast cycling blasts relative to HKG. Blasts were sorted using flow cytometry following seven day treatment with 5nM Dexamethasone.

DRAFT

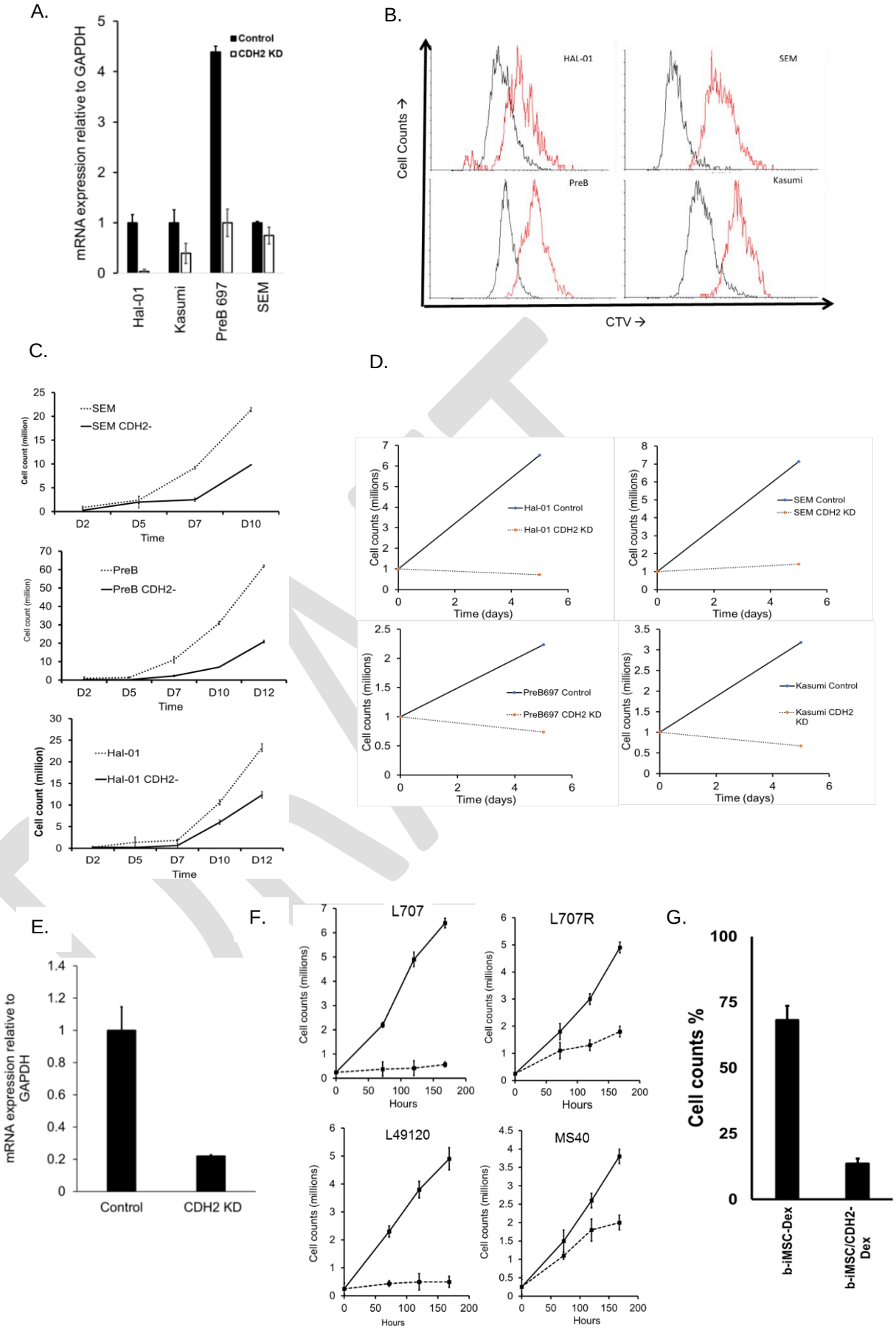
A.
mRNA expression relative to GAPDH
Control
CDH2 KD
Hal-01
Kasumi
PreB 697
SEM
B.
Cell Counts →
HAL-01
SEM
PreB
Kasumi
CTV →
C.
Cell count (million)
SEM
SEM CDH2-
PreB
PreB CDH2-
Hal-01
Hal-01 CDH2-
Time
D2
D5
D7
D10
D12
D.
Cell counts (millions)
Hal-01 Control
Hal-01 CDH2 KD
SEM Control
SEM CDH2 KD
PreB697 Control
PreB697 CDH2 KD
Kasumi Control
Kasumi CDH2 KD
Time (days)
E.
mRNA expression relative to GAPDH
Control
CDH2 KD
F.
L707
L707R
L49120
MS40
Cell counts (millions)
Hours
G.
Cell counts %
b-iMSC-Dex
b-iMSC/CDH2-Dex

Figure 4. CDH2 drives cancer proliferation and reduces sensitivity against Dexamethasone A. CDH2 levels in leukaemia cell lines following lentiviral knockdown. B. Cell generational tracing curves in 4 different leukemia cell lines following CDH2 knockdown. Black = empty vector control. Red = CDH2 knockdown C. Leukemic cell proliferation in three different acute lymphoblastic leukaemia cell lines following CDH2 knockdown [against empty vector control]. D. Cells counts of CDH2 knockdown and empty vector control cell lines on iANG. Feeder dependence was achieved by conducting co-cultures in the absence of FBS and at a reduced leukaemia cell density of 10,000 cells/ml. Furthermore, under these altered culture conditions the leukaemia cells failed to survive on iMSC. E. CDH2 mRNA levels in control iMSC and CDH2, knockdown, KD iMSC (iMSCCDH2-). F. Cell counts of three different patient leukemia samples on iMSC (standard line) and $iMSC^{CDH2-}$(dotted line). G. Cell counts of patient leukemia cells on $iMSC^{CDH2-}$ with and without 5 nM dexamethasone.

DRAFT

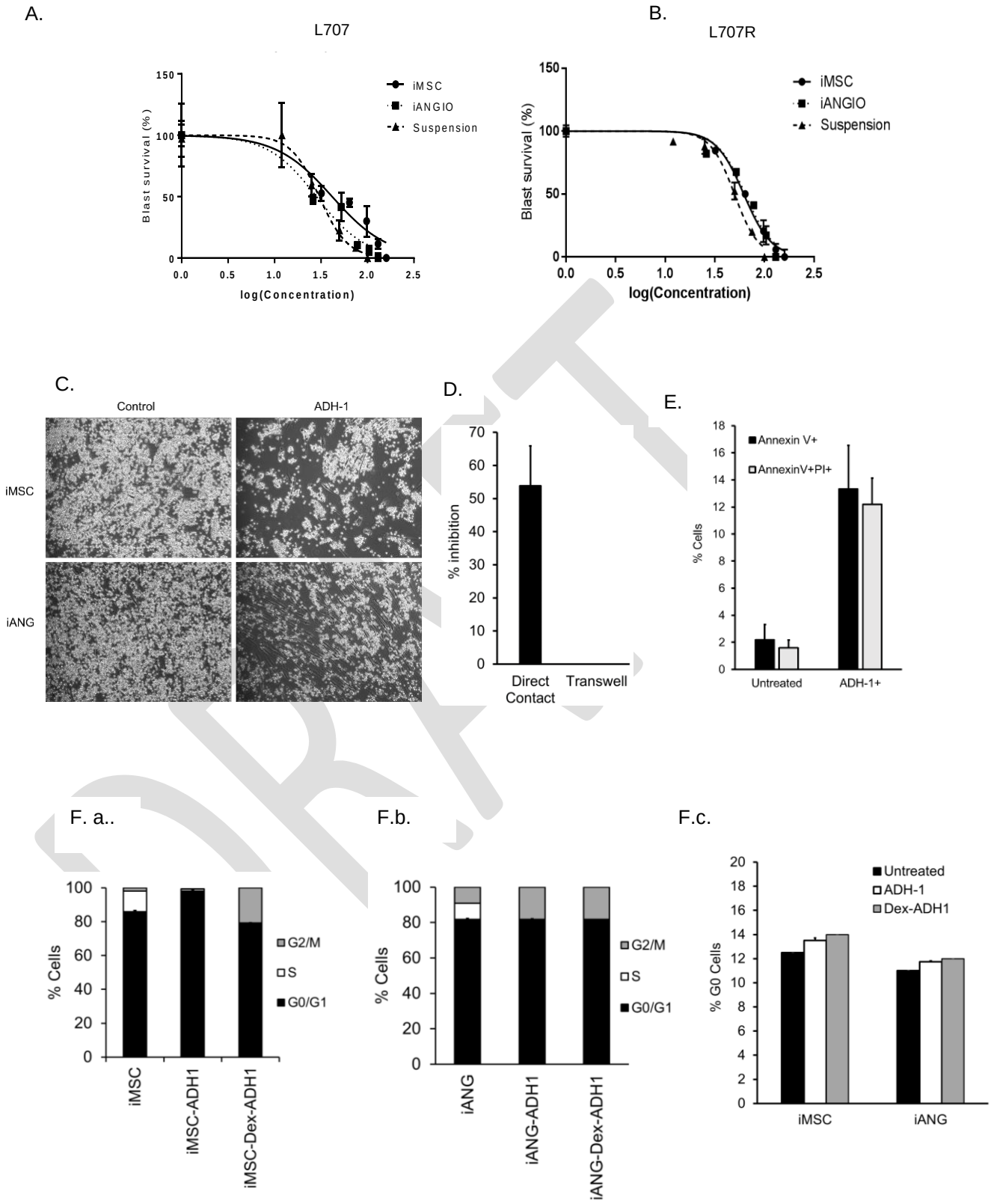
A.
L707
Blast survival (%)
log(Concentration)
iMSC
iANGIO
Suspension
B.
L707R
Blast survival (%)
log(Concentration)
iMSC
iANGIO
Suspension
C.
Control
ADH-1
iMSC
iANG
D.
% inhibition
Direct Contact
Transwell
E.
Annexin V+
AnnexinV+PI+
% Cells
Untreated
ADH-1+
F. a..
% Cells
G2/M
S
G0/G1
iMSC
iMSC-ADH1
iMSC-Dex-ADH1
F.b.
% Cells
G2/M
S
G0/G1
iANG
iANG-ADH1
iANG-Dex-ADH1
F.c.
Untreated
ADH-1
Dex-ADH1
% G0 Cells
iMSC
iANG

5. CDH2 antagonist ADH-1 a repurposed compound is identified to show high efficacy on a wide range of patient derived leukaemia cells A. ADH-1 dose response curves in patient leukemia samples from a patient at diagnosis and B. relapse. C. Adherent patient blasts on iMSC and iANG following treatment with ADH-1. D. % inhibition (cell counts) of blasts following ADH-1 treatment on direct contact cultures [iMSC] and in transwell cultures E. Annexin V PI flow cytometry analysis in patient blasts following treatment with ADH-1. F. a-c. RNA and DNA content analysis using flow cytometry in primary blasts following treatment with ADH-1 in a. iMSC and b. iANG co-cultures Column graphs show % cells in S and G0 phase following treatment with ADH-1. c. % G0 cells in co-cultures following treatment with ADH-1

DRAFT

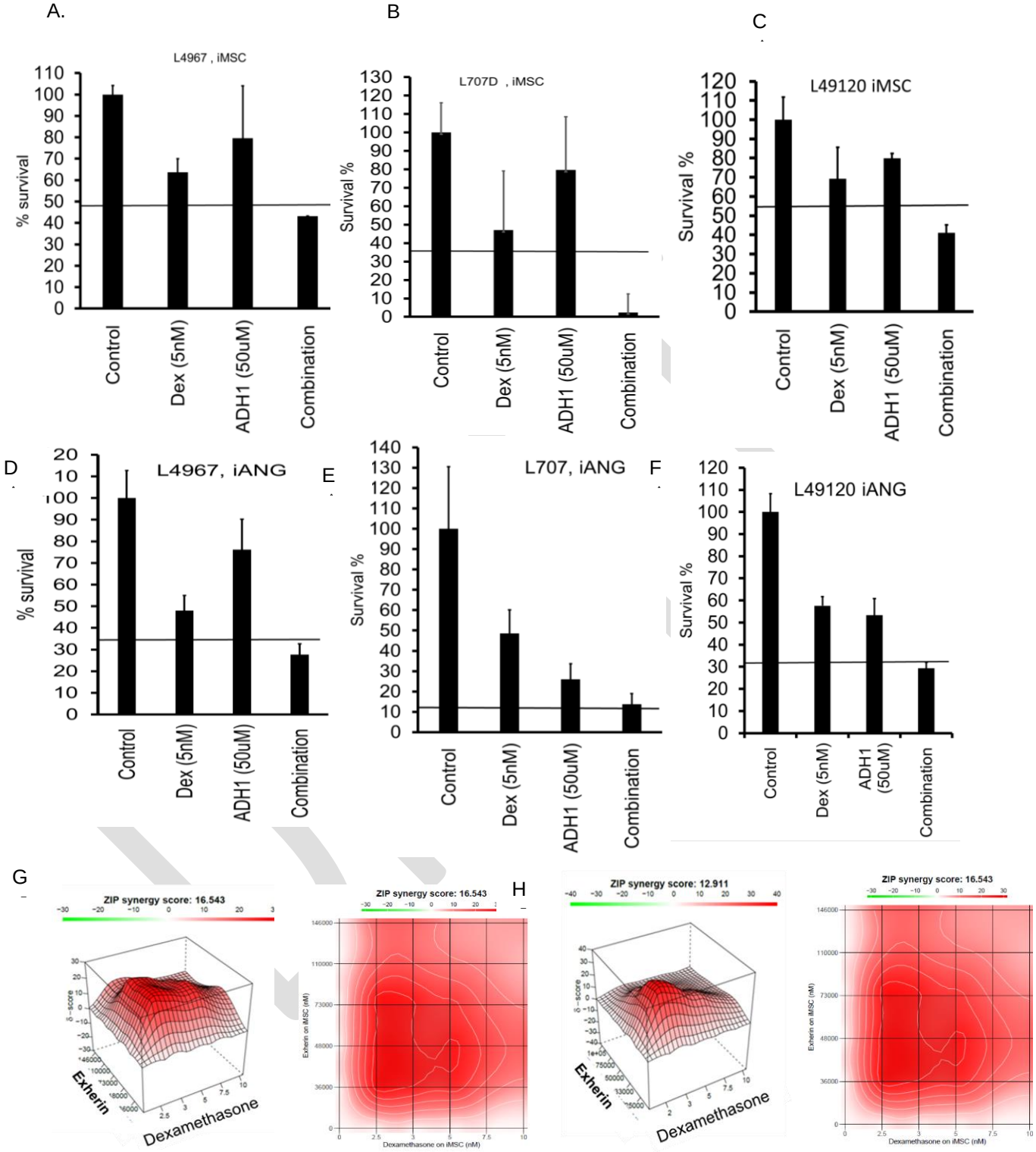
A.
L4967 , iMSC
% survival
Control
Dex (5nM)
ADH1 (50uM)
Combination
B
L707D , iMSC
Survival %
C
L49120 iMSC
D
L4967, iANG
E
L707, iANG
F
L49120 iANG
G
ZIP synergy score: 16.543
Exherin
Dexamethasone
H
ZIP synergy score: 12.911
Exherin on iMSC (nM)
Dexamethasone on iMSC (nM)

Figure 6. ADH-1 demonstrates in vitro synergy in combination with Dexamethasone. % survival following treatment with Dexamethasone, ADH-1 and combination in three different patient samples: A. L4967 B. L707D and C. L49120. On iMSC and D-F on iANG. Horizontal line depicts the expected combined effect as per the Bliss independence model. G. Synergy landscapes and ZIP synergy scores of ADH-1/Dex on primary patient blasts in iMSC and H. iANG co-cultures.

DRAFT

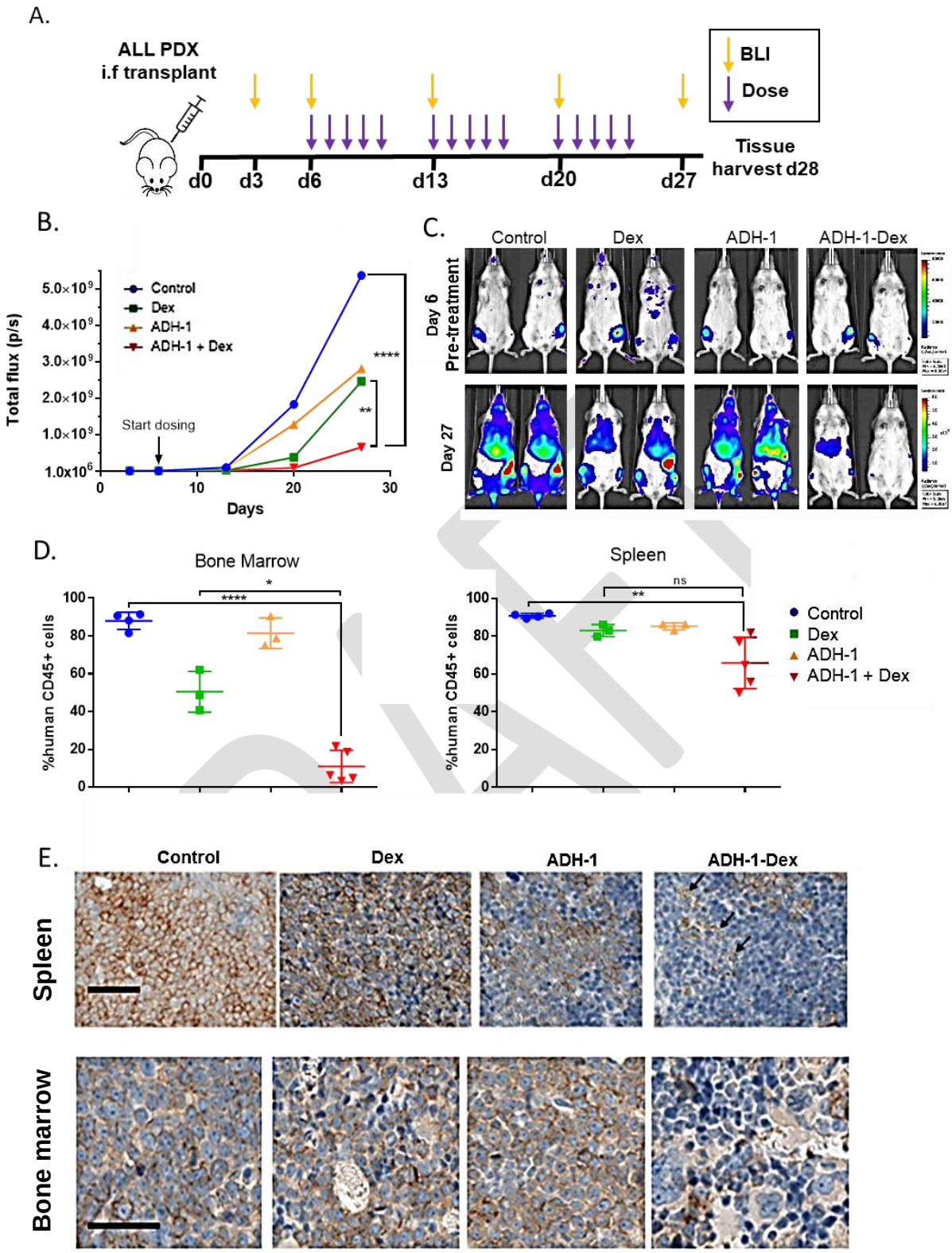
A.
ALL PDX
i.f transplant
BLI
Dose
Tissue
harvest d28
d0
d3
d6
d13
d20
d27
B.
Total flux (p/s)
Control
Dex
ADH-1
ADH-1 + Dex
Start dosing
Days
C.
Control
Dex
ADH-1
ADH-1-Dex
Day 6
Pre-treatment
Day 27
D.
Bone Marrow
Spleen
%human CD45+ cells
ns
Control
Dex
ADH-1
ADH-1 + Dex
E.
Control
Dex
ADH-1
ADH-1-Dex
Spleen
Bone marrow

Figure 7. ADH-1 potentiates dexamethasone sensitivity *in vivo*. A. The *in vivo* efficacy study design. Mice were dose interperitoneally with either, saline vehicle (control), 3mg/kg dexamethasone (Dex), 200mg/kg ADH-1 or ADH-1 Dex combined, 1x daily, 5x weekly for 3 weeks (15 doses). B. Mean whole-body total flux measurements from bioluminescent imaging of each treatment group. C. Representative luminescence images of mice before and after treatment. Mice at each time point are show with identical luminescence scale for comparison. Leukaemic blasts are present in the femurs of all mice at the start of treatment. Signal spreads to bone marrow sites, liver and spleen in control mice whereas signal is barely visible in ADH1-Dex controls. D. Leukaemic engraftment in harvested bone marrow and spleen measured by flow cytometry of labelled harvested cells. Human CD45+ cells are shown as a % total CD45+ cells (mouse and human cells). Lines indicate mean and SE, symbols for individual mice. 1 way ANOVA, ns not significant, * $p<0.05$, ** $p<0.005$, **** $p<0.00005$. E. Human CD19 Immunohistochemistry on sections of spleen and bone harvested from mice. Mice treated with ADH-1/Dex combination have few CD19 stained cells and have areas of punctate staining indicative of cell debris (arrows). Scale bar = 50µm.

DRAFT

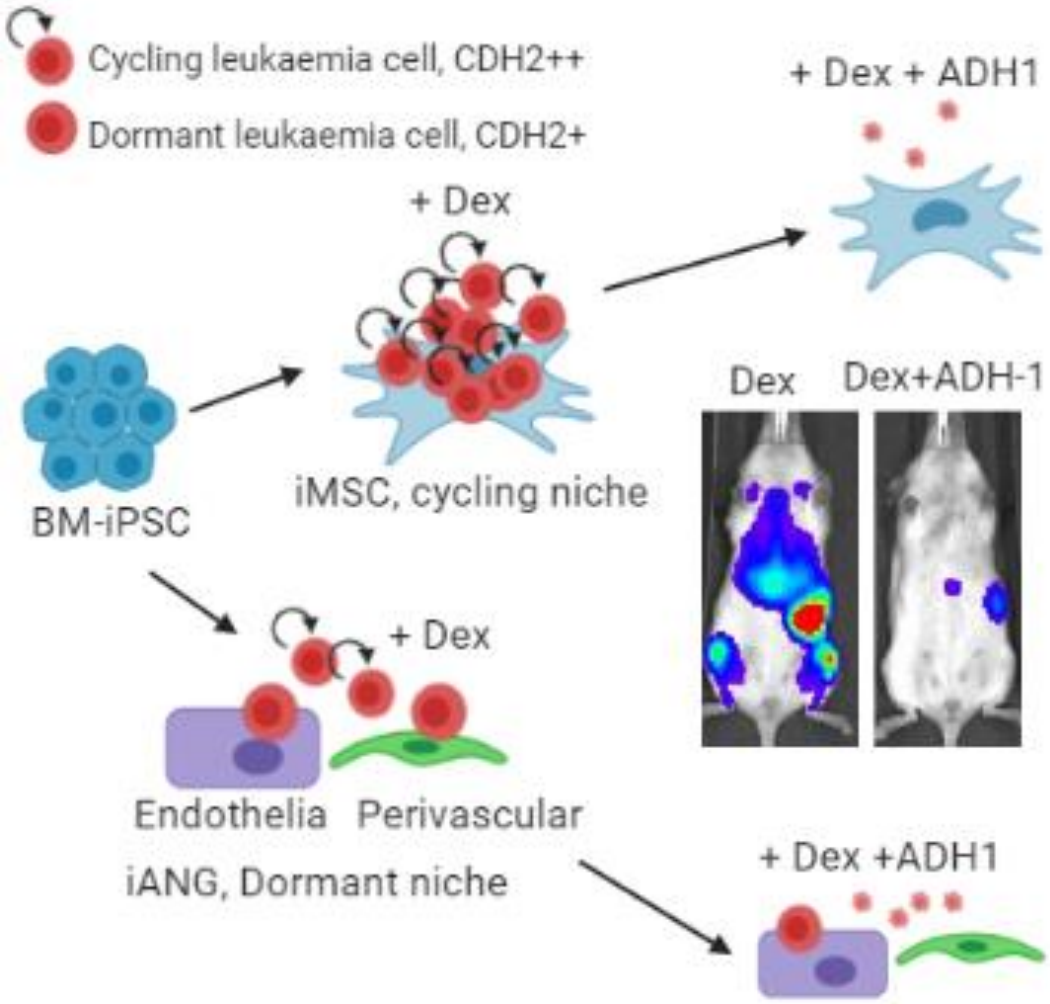
Cycling leukaemia cell, CDH2++
Dormant leukaemia cell, CDH2+
+ Dex
+ Dex + ADH1
BM-iPSC
iMSC, cycling niche
Dex
Dex+ADH-1
+ Dex
Endothelia
Perivascular
iANG, Dormant niche
+ Dex +ADH1

Figure 8. Summary. Proposed schematic of CDH2 mediate leukaemia proliferation and Dexamethasone resistance. BM-iPSC derived MSC [iMSC] and angiogenic cells [endothelia and perivascular, together iANG] support patient-derived leukaemia cells. iMSC chiefly supports actively cycling blasts while iANG support a population of cells that are dormant. Resistance against dexamethasone is seen on both these niche constituent cell types which suggests that cycling cells may also be potentially resistant to dexamethasone. The iMSC primed cycling cells upregulate CDH2 and the CDH2 antagonist ADH1 shows high efficacy in vivo both as a single agent and in combination with Dexamethasone.

DRAFT